RSC Advances

ROYAL SOCIETY OF CHEMISTRY

www.rsc.org/advances

Journal Name

COMMUNICATION

Confined Polymerization: Catalyzed Synthesis of High T_m, Nanofibrous Polyethylene within Porous Polymer Microspheres†

Received 00th January 20xx,
Accepted 00th January 20xx

DOI: 10.1039/x0xx00000x

www.rsc.org/

Kui Wang,[a,b] Jinhua Lei,*[a] and Guangyuan Zhou*[a]

Crystalline nanofibers of linear polyethylene were formed through ethylene confined polymerization with porous polymer microsphere-supported titanocene. Polyethylene nanofibers (<70 nm) aggregated to form intertwined thicker fibers (300 nm to 22 μm). The obtained PE has a high M_w and T_m. Interestingly, the high T_m (142.4 °C) was maintained in the second stage of heating.

Over the last 50 years several large advances have been achieved in polymer chemistry; one of these advances is the use of metallocene catalysts for olefin polymerization.[1-3] This discovery re-ignited scientific interest in the field of single-site catalysis, with metallocenes at its vanguard. However, the use of homogeneous metallocenes also has some disadvantages, such as high methylaluminoxane (MAO) /metallocene molar ratio, bad polymer morphology and reactor fouling, and activity loss.[4-5]

Amorphous and porous SiO_2 at present is a good support for metallocenes because of its high surface area, porous microstructure, good mechanical property, stability and inertness under reaction and processing condition.[6-7] Recently, with the development of nanotechnology, polymerization in a micro- or nano-reactor has attracted considerable interest.[8-10] Polymerization in confined space is a powerful method for controlling polymer architecture over various hierarchical levels, such as microstructure, morphology, and nano- and micro-object generation, thus accessing properties that are distinctly different from those of the corresponding bulk phases.[11-12] For example, polymers synthesized in nanoscale pores reportedly possess high electrical conductivity and high modulus.[13]

Inorganic mesoporous materials are good nanoreactors for olefin polymerization. However, the acidic supports with reactive surfaces can cause catalyst deactivation.[14-15] Meanwhile, inorganic supports commonly show rigid and polar surface structures as opposed to hydrocarbon materials that provide close analogs to the environment prevailing in homogeneous polymerization.[12-13, 16-17] Hence, Roscoe et al.[18] designed insoluble polymer particles with the appropriate catalyst to facilitate a nominally heterogeneous polymerization in a microscopically homogeneous "solution-like" environment.

To combine the advantages of polymerization in nanoreactors and organic supports, we have designed and synthesized a porous polymer microspheres (PPMs) support and it was further used as support for Ziegler–Natta catalyst as well as Cp_2ZrCl_2 catalyst in ethylene polymerization.[19-20] PPM-supported Ziegler–Natta catalyst served as a nanoreactor in ethylene polymerization, while the PPM-supported Cp_2ZrCl_2 catalyst did not. This result can be attributed to the different activities of these two catalysts. The starting activity of PPM-supported Cp_2ZrCl_2 catalyst was very high, and the support was broken into fragments at the beginning of the polymerization. In order to get a stable and controlled confined space polyerization with PPM-supported metallocene catalyst, a lower activity metallocene catalyst Cp_2TiCl_2 was selected in this work.

The cyano-functionalized PPMs have a tri-modal pore structure of interconnected macropores, mesopores and micropores, and have a high surface area in the dry state.[20] The morphologies of PPMs and PPM-supported catalyst were shown in Fig. S1 (Supporting Information), the spherical shape of the PPMs was maintained after Cp_2TiCl_2 loading. The structure parameters of the PPMs and PPM-supported catalyst were demonstrated in Table 1. The N_2 adsorption-desorption results indicated that the interconnected pore structure was not destroyed after catalyst loading. The S_{BET} and V_p of the PPM-supported catalyst apparently decreased from 278 m^2/g to 25 m^2/g, and from 0.418 cm^3/g to 0.083 cm^3/g, respectively, compared with those of the PPMs. Conversely, the average d_p increased from 9.05 nm to 25.4 nm, this can be attributed to the decrease of micropores which were obstructed by the supported catalyst. This deduction can be further confirmed by the pore width distribution curves as shown in Fig. 1. ICP-AES result showed that the Ti and Al contents of the supported catalyst were 0.0899 and 2.861 mmol/g, respectively (Table 1).

[a] Key Laboratory of Polymer Ecomaterials, Changchun Institute of Applied Chemistry, Chinese Academy of Sciences, Renmin Street 5625, Changchun, Jilin, 130022, China.
[b] University of Chinese Academy of Sciences, Beijing, 100049, China.

† Electronic Supplementary Information (ESI) available: See DOI: 10.1039/x0xx00000x

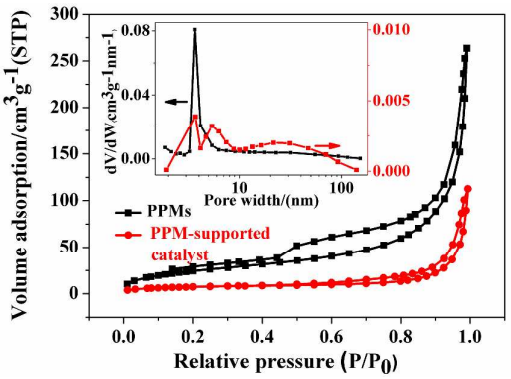

Fig. 1 The N_2 adsorption–desorption isotherms and pore size distributions for PPMs and PPM-supported catalyst.

Table 1 The structure parameters[a] of the PPMs with/without catalyst and the Ti and Al contents of the supported catalyst.

Sample	S_{BET} (m^2/g)	V_p (cm^3/g)	d_p (nm)	Ti (mmol/ g-cat)	Al (mmol/ g-cat)
PPMs	278	0.418	9.05	/	/
PPM-supported catalyst	25	0.083	25.4	0.0899	2.861

[a] The BET specific surface area (S_{BET}), specific pore volume (V_p), and average pore diameter (d_p) were obtained from BJH adsorption data.

XPS and FT-IR were used to investigate the formation process of the polymer supported catalyst (Fig. S2). The cyano group (2240 cm^{-1}) was partially transferred to the imine group (1635 cm^{-1}). This result demonstrated the strong interaction between the PPMs and the catalyst. Fig. S2b showed that a 0.5 eV increase occured in binding energy of N_{1s} of the Modified PPMs compared with that of the PPMs. This demonstrated that N of the support has a strong interaction with MMAO. Fig. S2c showed that the binding energy of $Ti_{2p3/2}$ and $Ti_{2p1/2}$ in the PPM-supported catalyst were 458.0 eV and 464.0 eV. It increased 0.5 eV when compared with homogenerous Cp_2TiCl_2 reported in literature [21] and a similar phenomenon was also observed in ethylene polymerization by PPM-supported Cp_2ZrCl_2 catalyst (increased 0.7 eV)[20] and $MgCl_2$ supported $TiCl_4$ catalyst (increased 1.3 eV).[22] That confirms titanium has been transferred to a cationic active species. Thus, the structure of the PPM-supported catalyst formed in the supporting processes can be postulated as in Scheme S1.

Table 2 Results of ethylene polymerizations with the PPM-supported and homogeneous Cp_2TiCl_2 catalytic systems.

Run	Activity[a]	T_{m1}[b]/°C	X_c%	T_{m2}[c]/°C	X_c%	Tc/°C	M_w[d]	PDI
1	28.4	144.1	45	142.4	35	110.1	33.8	2.09
2	80.6	143.8	42	142.2	38	108.2	24.2	2.09
3[#]	365.8	138.6	70	137.7	52	113.1	22.4	2.21

Polymerization conditions: in a 0.1 L autoclave, 60 mL hexane (# homogeneous Cp_2TiCl_2 catalyst); polymerization time: 0.5 h; polymerization pressure: 5 atm; polymerization temperature: 50 °C.
[a] kg of PE/(mol of Ti h atm).
[b] the first T_m of DSC scan.
[c] the second T_m of DSC scan.
[d] Weight-average molecular weight (M_w): $\times 10^4$ g/mol.

Consequently, ethylene polymerization was carried out with PPM-supported Cp_2TiCl_2, and the results were shown in Table 2. The polymerization activities were lower than corresponding PPM-supported Cp_2ZrCl_2 catalyst as we expected.[20]
The M_w of the PE produced by the PPM-supported catalyst ranged within of 242 000–338 000 g /mol PE (Fig. S5), which was higher than that of the PE obtained by the homogeneous catalyst in the literature.[23] Ethylene polymerization synthesized by PPM-supported Ziegler-Natta catalyst was also carried out, and their M_w and PDI are 543 000 g /mol and 2.16, respectively. That result is consistent with ethylene confined polymerization by PPM-supported Cp_2TiCl_2 catalyst and the literatures about confined polymerization.[24-26]

PE nanofibers and microfibers with a diameter of 300 nm-22 μm were observed by SEM (Fig. 2a and 2b). The cross-section of the PE fibers were further studied. Fig. 2c showed that the nanofibers were consisted of thinner nanofibers (<1 μm), and Fig. 2d displayed the microfibers were consisted of nanofibers. This was a critical result of confined polymerization as was given in literatures.[25, 27]

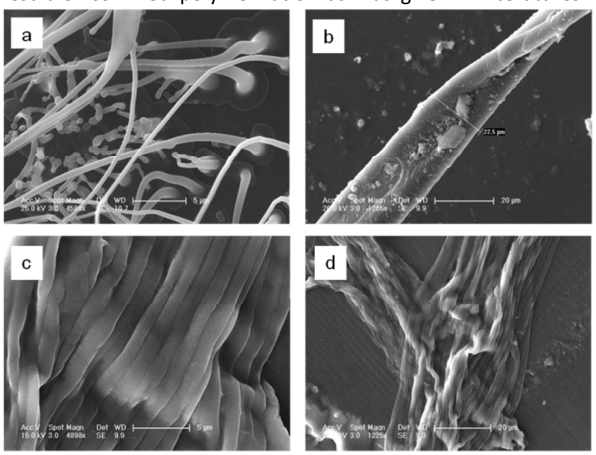

Fig. 2 The SEM micrographs of the PE samples produced by PPM-supported catalyst. (a-b), cross-section morphology of nanofibers (c) and microfibers (d). Scale bars: (a) 5 μm, (b) 20 μm, (c) 5 μm, and (d) 20 μm.

Table 3 DSC Results of the post-treated PE.

Run	trichlorobenzene boiled for 80 h at 180 °C	
	T_{m1}/°C	T_{m2}/°C
1(heterogeneous PE)	143.6	141.6
2(heterogeneous PE)	141.4	141.2
3(homogeneous PE)	136.4	137.6

The X-ray diffraction (XRD) spectra of the PE samples (Fig. S5a) showed that they were typical orthorhombic crystal structures.[28] The ^{13}C-NMR spectra (Fig. S5b) indicated that the resulting PE was a linear sequence of the repeating ethylene without any branch structures.

DSC results (Table 2 and Fig. S3) showed that the first scan melting point was very high (up to 144.1 °C). Unexpectedly, the high melting point was maintained in the second stage of heating and that high melting point was also observed in the polyethylene synthesized by PPM-supported Ziegler-Natta catalyst (143.8 °C), which was higher than that of PE produced by homogeneous Cp_2TiC_2 catalyst (Run 3) and the PE reported in literatures (134~136 °C).[29-30] Such a high second scan T_m of nascent PE synthesized over heterogeneous catalysts has not been reported.

The change of X_c after first and second scans in Run 1 and Run 2 is similar to the literatures.[26, 29] That may be attributed to the formation of folded-chain lamellar crystal structure and the influence of supports.[16, 26, 29]

The resultant PE was also boiled for 80 h by trichlorobenzene at 180 °C (Table 3). After that treatment the melting point of PE produced by PPM-supported catalyst is still higher (141.6 °C) than that of homogenous PE (137.6 °C). So that we can deduce that the high T_m of PE produced by PPM-supported catalyst is their fundamental character.

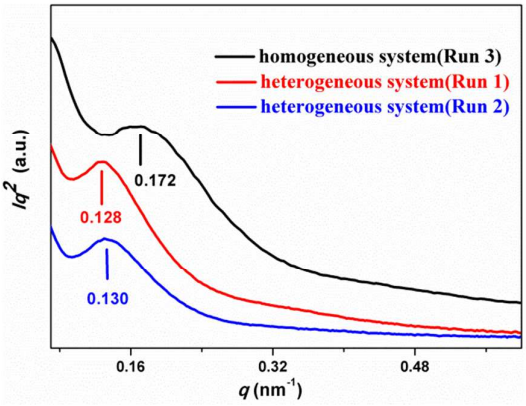

Fig. 3 The one-dimensional SAXS spectra of the PE samples prepared with PPM-supported and homogeneous catalytic systems.

Table 4 The d_a, d_{ac} and d_c of PE synthesized by different catalytic systems.

catalytic systems	T_{m2}/°C	q	d_{ac}[a]/nm	X_c%	d_c[b]/nm
homogeneous PE (Run 3)	137.2	0.172	36.5	52	19.0
hetrogeneous PE (Run 1)	142.4	0.128	49.1	35	17.2
hetrogeneous PE (Run 2)	142.2	0.130	48.3	38	18.4

[a] $d_{ac}=2\pi/q$.; [b] $d_c=d_{ac}* X_c$.

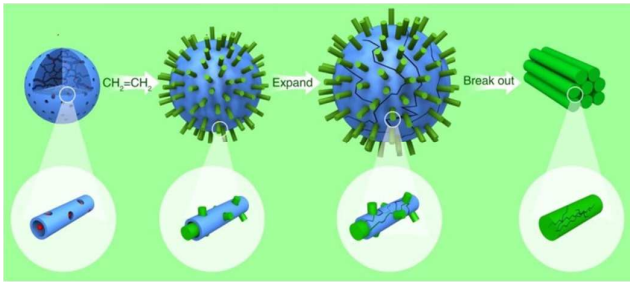

Scheme 1 Synthesis of PE nanofibers in PPMs reactors.

The PE with high T_m were further investigated by Small-angle x-ray scattering (SAXS). Fig. 3 and Table 4 showed the one-dimensional SAXS profiles and the correlation function, respectively. The thicknesses of amorphous layers (d_a) and crystalline lamellae (d_c) of PE were derived from the SAXS and DSC results.[31-32]

The effect of lamellar thickness (d_c) and surface free energy (σ_e) on the melting point (T_m) can be represented by the Gibbs-Thompson equation (Equation 1).

$$T_m = T_m^0\left(1-\frac{2\sigma_e}{d_c\Delta H_f^0}\right) \quad (1)$$

Where T_m^0 is the equilibrium melting point, ΔH_f^0 is the enthalpy of fusion per unit volume. In Table 4 the d_c of PE were almost not changed in different catalytic systems. The Gibbs-Thompson equation indicates that the smaller the surface free energy is, the higher the melting point becomes. The high T_m in Run 1 and Run 2 was owing to the low surface free energy σ_e. That might be attributed to the influence of the support. The PPMs support has a tri-modal pore structure of interconnected macropores, mesopores and micropores, then the interconnected pore structure leads to a large content of entanglement chains of PE produced by PPM-supported Cp_2TiCl_2 catalyst.

Clearly, crystallites in homogeneous PE possess much more chain ends than that of heterogeneous PE due to their entanglement chains. During the heating process, the mobility devoted by a large content of entanglement chains in heterogeneous PE (Run 1 and 2) was evidently less intensive than the one contributed by chain ends in homogeneous PE (Run 3), leading to a lower surface free energy of stable crystallites in heterogeneous PE than the one in homogeneous PE. Moreover, the entanglement chains are difficult to unfold even they are boiled for 80 h at high temperature (Table 3). Hence, the entanglement chains in heterogeneous PE (Run 1 and 2) may be the reason that maintained the high T_m after first and second scans. That is described in Men's study.[31]

Basing on the above results, nascent linear PE with high T_m and nanofiber structure was obtained, ethylene polymerization with porous polymer supported titanocene performed as critical confined polymerization. Scheme 1 shows the concluded mechanism of the confined polymerization with the PPM-supported titanocene. In situ confined polymerization allowed the synthesis of PE nanofibers， then the nanofibers aggregated to form thick PE nanofibers and even microfibers.

In summary, Cp_2TiCl_2 catalyst was supported into porous polymer microspheres (PPMs), and then it was used for ethylene

polymerization. Linear PE with high T_m and nanofiber structure was obtained, ethylene polymerization with porous polymer supported titanocene performed as a critical confined polymerization. The high T_m in the second scan was owing to the low surface free energy σ_e. Moreover, the significant high T_m of obtained polyethylene may expand the application areas of polyethylene in some content.

EXPERIMENTAL

For equipment and materials, syntheses of PPMs, PPM-supported catalyst, and ethylene polymerization and characterization, please see Supporting Information.

ACKNOWLEDGEMENTS

This work was supported by The National Natural Science Foundation of China for project No. 51373163, No. 21104073.

Notes and references

1. G. W. Coates, *Chem. Rev.*, 2000, **100**, 1223-1252.
2. W. Kaminsky, *Macromolecular Chemistry and Physics*, 2008, **209**, 459-466.
3. W. Kaminsky, R. Engehausen, K. Zoumis, W. Spaleck and J. Rohrmann, *Makromolekulare Chemie-Macromolecular Chemistry and Physics*, 1992, **193**, 1643-1651.
4. G. G. Hlatky, *Chem. Rev.*, 2000, **100**, 1347-1376.
5. G. Fink, B. Steinmetz, J. Zechlin, C. Przybyla and B. Tesche, *Chem. Rev.*, 2000, **100**, 1377-1390.
6. S. Collins, W. M. Kelly and D. A. Holden, *Macromolecules*, 1992, **25**, 1780-1785.
7. C. Janiak and B. Rieger, *Angewandte Makromolekulare Chemie*, 1994, **215**, 47-57.
8. A. Comotti, S. Bracco, M. Mauri, S. Mottadelli, T. Ben, S. Qiu and P. Sozzani, *Angewandte Chemie-International Edition*, 2012, **51**, 10136-10140.
9. T. Uemura, N. Yanai and S. Kitagawa, *Chemical Society Reviews*, 2009, **38**, 1228-1236.
10. K. Tajima and T. Aida, *Chemical Communications*, 2000, 2399-2412.
11. C. R. Martin and P. Kohli, *Nature Reviews Drug Discovery*, 2003, **2**, 29-37.
12. A. Arinstein, M. Burman, O. Gendelman and E. Zussman, *Nature Nanotechnology*, 2007, **2**, 59-62.
13. H. W. Lee, J. S. Chung and K. Y. Choi, *Polymer*, 2005, **46**, 5032-5039.
14. X. Dong, L. Wang, G. Jiang, Z. Zhao, T. Sun, H. Yu and W. Wang, *Journal of Molecular Catalysis A: Chemical*, 2005, **240**, 239-244.
15. K. S. Lee, C. G. Oh, J. H. Yim and S. K. Ihm, *J. Mol. Catal. A-Chem.*, 2000, **159**, 301-308.
16. S. Nair, P. Naredi and S. H. Kim, *The Journal of Physical Chemistry B*, 2005, **109**, 12491-12497.
17. C. Guo, D. Zhang, F. Wang and G.-X. Jin, *Journal of Catalysis*, 2005, **234**, 356-363.
18. S. B. Roscoe, J. M. J. Frechet, J. F. Walzer and A. J. Dias, *Science*, 1998, **280**, 270-273.
19. J. H. Lei, D. L. Li, H. H. Wang and G. Y. Zhou, *Polymer*, 2011, **52**, 602-605.
20. J. Lei, D. Li, H. Wang, Z. Wang and G. Zhou, *Journal of Polymer Science Part a-Polymer Chemistry*, 2011, **49**, 1503-1507.
21. F. Garbassi, L. Gila and A. Proto, *J. Mol. Catal. A-Chem.*, 1995, **101**, 199-209.
22. D. Fregonese, A. Glisenti, S. Mortara, G. A. Rizzi, E. Tondello and S. Bresadola, *J. Mol. Catal. A-Chem.*, 2002, **178**, 115-123.
23. W. Kaminsky, M. Miri, H. Sinn and R. Woldt, *MAKROMOLEKULARE CHEMIE-RAPID COMMUNICATIONS*, 1983, **4**, 417-421.
24. S. Park and I. S. Choi, *Advanced Materials*, 2009, **21**, 902-905.
25. K. Y. Choi, J. J. Han, B. He and S. B. Lee, *Journal of the American Chemical Society*, 2008, **130**, 3920-3926.
26. D. Li, J. Lei, H. Wang, M. Jiang and G. Zhou, *Polymer bulletin*, 2012, **68**, 1565-1575.
27. X. Dong, L. Wang, J. Wang, J. Zhou and T. Sun, *The Journal of Physical Chemistry B*, 2006, **110**, 9100-9104.
28. S. Krimm and A. V. Tobolsky, *Journal of Polymer Science*, 1951, **7**, 57-76.
29. Z. B. Ye, S. P. Zhu, W. J. Wang, H. Alsyouri and Y. S. Lin, *J. Polym. Sci. Pt. B-Polym. Phys.*, 2003, **41**, 2433-2443.
30. K. Kageyama, J.-i. Tamazawa and T. Aida, *Science*, 1999, **285**, 2113-2115.
31. Y. Lu, Y. Wang, Z. Jiang and Y. Men, *ACS Macro Letters*, 2014, **3**, 1101-1105.
32. Y. Wang, Y. Lu, Z. Jiang and Y. Men, *Macromolecules*, 2014, **47**, 6401-6407.